Analysis of the Respiratory Dynamics During Normal Breathing by Means of Pseudophase Plots and Pressure–Volume Loops

Clara M. Ionescu, *Member, IEEE*, J. A. Tenreiro Machado, *Senior Member, IEEE*, and Robin De Keyser

***Abstract*—This paper reports on the analysis of tidal breathing patterns measured during noninvasive forced oscillation lung function tests in six individual groups. The three adult groups were healthy, with prediagnosed chronic obstructive pulmonary disease, and with prediagnosed kyphoscoliosis, respectively. The three children groups were healthy, with prediagnosed asthma, and with prediagnosed cystic fibrosis, respectively. The analysis is applied to the pressure–volume curves and the pseudophase-plane loop by means of the box-counting method, which gives a measure of the area within each loop. The objective was to verify if there exists a link between the area of the loops, power-law patterns, and alterations in the respiratory structure with disease. We obtained statistically significant variations between the data sets corresponding to the six groups of patients, showing also the existence of power-law patterns. Our findings support the idea that the respiratory system changes with disease in terms of airway geometry and tissue parameters, leading, in turn, to variations in the fractal dimension of the respiratory tree and its dynamics.**

***Index Terms*—Correlation, delay, forced oscillation, fractal dimension, geometrical mapping, homothety factor, lung function test, phase plot, respiratory impedance.**

I. Introduction

THE study of fractional order systems has received considerable attention lately [40], due to the fact that many physical systems are well characterized by fractional models [36]. With the success in the synthesis of real noninteger differentiators, the emergence of new electrical elements, and the design of fractional controllers [31], [39], fractional calculus has been applied in a variety of dynamical processes [42]. The advantage of fractional order mathematical models is that they can be used to make a more accurate description and to give a deeper insight into the physical processes underlying long-range memory behaviors. In previous works, it was demonstrated that the respiratory system has fractal dynamics and constitutes a good test-bed for their study [19], [22]. Furthermore, long-range (power law) correlations have confirmed the presence of fractal scaling and dependence on the respiratory dynamics much in the past (i.e., several breathing periods earlier) [17], [18]. It has been shown that such fractal scaling exponents of long-range correlations in breathing dynamics are varying with age and gender [35]. These probing studies are the pioneering steps taken toward a full understanding of these complex nonstationary characteristics of the respiratory signals.

Previous work has shown that the lung parenchyma behaves as a long-memory system with viscoelastic properties [4], [38]. The typical structure of the healthy respiratory system has also been shown to be well captured by lumped models with fractional order integrals and derivatives [20], [22]. Intrinsically, fractional calculus incorporates a memory-time property because it captures the dynamic phenomena involved during all the time history of a system [42]. A delay differential equation is a description where the evolution of a system at a certain time depends on the state of the system at an earlier time [9], [11], [15]. Such a relation is usually graphically analyzed by means of phase plots. Hence, intuitively, there must exist a relationship between the information extracted from the phase plots and fractional calculus. This motivates our interest in evaluating the dynamic patterns of the breathing, since it may provide useful insight into relating the changes in airway structure and tissue properties with the changes in the respiratory dynamics.

The pseudophase space is used to analyze signals with nonlinear behavior. For the 2-D case, it is called pseudophase plane (PPP) [30]. To reconstruct the PPP, it is necessary to find the adequate time lag between the signal and one delayed image of the original signal. Since PPP proved successful in various technical applications, we propose the use of PPP tools to analyze data from lung function tests in healthy subjects and in patients with respiratory disorders. The novelty of the proposed methodology is to combine the information from PPP with the corresponding fractal dimension computed using the box-counting method. In this way, the fractal dynamics of the respiratory system can be assessed and further analyzed.

One of the most common clinical features extracted from lung function tests is the air-pressure and the airflow variations during forced breathing or during breathing at rest. A standard measure of the work of breathing in lung function analysis is obtained by means of pressure–volume (PV) loops acquired during spirometry (i.e., by means of forced breathing maneuvers). The data used in this application have been acquired in

Manuscript received January 11, 2011; revised August 6, 2011; accepted January 13, 2012. Date of publication March 2, 2012; date of current version December 12, 2012. This work was supported by the Flanders Foundation for Scientific Research (FWO). This paper was recommended by Associate Editor G. C. Calafiore.

C. M. Ionescu and R. De Keyser are with the Department of Electrical Energy, Systems, and Automation, Ghent University, B9052 Ghent, Belgium (e-mail: ClaraMihaela.Ionescu@UGent.be; Robain.DeKeyser@UGent.be).

J. A. Tenreiro Machado is with the Department of Electrical Engineering, Porto Superior Institute of Engineering, Polytechnic Institute of Porto, 4200-072 Porto, Portugal (e-mail: jtm@isep.ipp.pt).

Color versions of one or more of the figures in this paper are available online at http://ieeexplore.ieee.org.

Digital Object Identifier 10.1109/TSMCA.2012.2187888

TABLE I
BIOMETRIC AND SPIROMETRIC PARAMETERS OF THE INVESTIGATED ADULT SUBJECTS. VALUES ARE PRESENTED AS MEAN ± STANDARD DEVIATION; % PRED: PREDICTED ACCORDING TO THE ASYMPTOMATIC SUBJECTS OF THE PRESENT STUDY; FVC: FORCED VITAL CAPACITY; FEV_1: FORCED EXPIRATORY VOLUME IN 1 S. KS–KYPHOSCOLIOSIS; COPD–CHRONIC OBSTRUCTIVE PULMONARY DISEASE

ADULTS	**Healthy**	**KS**	**COPD**
female	**12**	**2**	**0**
male	**30**	**22**	**39**
Age [years]	27 ± 2	62 ± 10	64 ± 3
Height [m]	1.73 ± 0.27	1.55 ± 0.08	1.73 ± 0.14
Weight [kg]	69 ± 5.6	63 ± 15	79 ± 12
FVC [%pred]	-	33 ± 14	84 ± 12
FEV_1 [%pred]	-	31 ± 11	38 ± 6

TABLE II
BIOMETRIC AND SPIROMETRIC PARAMETERS OF THE INVESTIGATED CHILDREN SUBJECTS. VALUES ARE PRESENTED AS MEAN ± STANDARD DEVIATION; % PRED: PREDICTED ACCORDING TO THE ASYMPTOMATIC SUBJECTS OF THE PRESENT STUDY; FVC: FORCED VITAL CAPACITY; FEV_1: FORCED EXPIRATORY VOLUME IN 1 S; FEF: FORCED EXPIRATORY FLOW; CF–CYSTIC FIBROSIS

CHILDREN	**Healthy**	**Asthma**	**CF**
female	**9**	**35**	**8**
male	**24**	**9**	**30**
Age [years]	9 ± 1	11 ± 4	14 ± 6
Height [m]	1.35 ± 0.05	1.40 ± 0.2	1.49 ± 0.15
Weight [kg]	32 ± 6	36 ± 15	40 ± 11
FEF/FVC [%pred]	-	85 ± 31	86 ± 9
FEV_1/FVC [%pred]	-	97 ± 1.2	95 ± 0.9

lung function tests during breathing at rest, namely, the forced oscillation technique (FOT) [33]. We aim to analyze six sets of patient data: healthy adults, adults prediagnosed with chronic obstructive pulmonary disease (COPD), adults prediagnosed with kyphoscoliosis (KS), healthy children, children prediagnosed with asthma, and children prediagnosed with pulmonary cystic fibrosis (CF).

This paper is organized as follows. Section II introduces the materials and methods employed in this paper. The breathing recordings from patients in time domain are presented for one patient in each group, along with information upon the various sets of data, biometric details of the population sets, and measurement protocol. A short description of the PV loops and the PPP technique employed here is given in the same section. Next, the processing of the information extracted from the PV loops and the PPP plots and the calculus of the fractal dimension follows, along with a power-law model structure. Section III presents the results and the feature analysis, while Section IV discusses the geometrical and clinical interpretation of the emerged results. Finally, a conclusion section summarizes the main outcome of this paper.

II. MATERIALS AND METHODS

A. Patients

There are six sets of patients available for analysis. We have both children and adult subjects, for each class of healthy and respiratory disorders. The biometric and spirometric details are given in Tables I and II for adults and children, respectively. Part of these groups of patients have been previously employed in a study on classification tools by means of multidimensional scaling [25], where we successfully mapped obstructive and restrictive pathologies in adult population. In the present study, we shall investigate a similar pool of patients, in our quest to find complementary tools to assess respiratory dynamics.

Some of the most commonly used lung function test measurements are performed during forced inspirations and forced expirations, i.e., spirometry. A person's vital capacity can be measured by a spirometer [32]. The combination of several physiological measurements can help make a diagnosis of the underlying lung disease. Forced vital capacity (FVC) is the maximum volume of air that a person can exhale after maximum inhalation. Another important measure in spirometry is the forced expired volume in 1 s (FEV_1). The FEV_1/FVC ratio is used in the diagnosis of *obstructive* and *restrictive* lung diseases, and normal values are approximately 80% [32]. In obstructive lung disease, the FEV_1 is reduced due to obstruction to air escape. Thus, the FEV_1/FVC ratio will be reduced. In restrictive lung disease, the FEV_1 and FVC are equally reduced due to fibrosis or to other lung pathology (not obstructive pathology). Thus, the FEV_1/FVC ratio should be approximately normal.

In this paper, all patients were *a priori* diagnosed based on standard lung function tests (spirometry, body plethysmography, and bronchoprovocation) and their medical history. However, for the sake of clarity, in this paper, we provided some of the most important spirometric parameters.

All measurements with the forced oscillation lung function testing device were done by the same person, applying the same protocol. For the other pulmonary tests, the existing trained clinical staff on each location was employed.

The measurements were approved by Ethical Committee Commissions at each location. The measurements in adult subjects were approved by the Ghent University Hospital in Belgium and Leon Daniello Hospital in Cluj-Napoca, Romania, for adults. The measurements in children were approved by the University Hospital Antwerp in Belgium. Written and/or oral consent was obtained from all participants and, in case of children, from both children and their parents.

1) Measurements in Adults: The **healthy adult group** evaluated in this study consists of 42 Caucasian volunteers (students) without a history of respiratory disease, whose lung function tests were performed in our laboratory.[1] Their selection was based on a questionnaire. Table I presents their biometric parameters. The respiratory impedance derived from the forced oscillation lung function test was validated against typical prediction values [34], [37]. The identified values from our measurements remained close to the predicted values and within the 95% confidence interval. The measurements were done over the period 2010–2011.

COPD denotes any disorder that persistently obstructs the bronchial airflow [2]. However, it mainly involves two related diseases: chronic bronchitis and emphysema. Both cause chronic obstruction of air flowing through the airways and in and out of the lungs. The obstruction is irreversible and progresses (becomes worse) over time.

[1] Ghent University, Ghent, Belgium.

The COPD group consisted of 39 Caucasian COPD-diagnosed patients under observation at the "Leon Daniello" Hospital. The majority of the patients were former coal miners from the Petrosani area in Romania. Their selection to the study was done based on the medical history and the recommendation from the clinical supervisor. Their biometric and spirometric parameters are given in Table I. The data presented from these patients have been collected in 2006 and, in part, analyzed by means of respiratory impedance in [21].

KS is a disease of the spine and its articulations, mostly beginning in childhood [29]. The deformation of the spine characteristically consists of a lateral displacement or curvature (scoliosis) or an anteroposterior angulation (kyphosis) or both (KS). The angle of the spinal curvature called *the angle of Cobb* determines the degree of the deformity and, consequently, the severity of the restriction.

The study on the KS group was approved by the local Ethics Committee of the Ghent University Hospital, and informed consent was obtained from all volunteers before inclusion in the study. It involved 24 data sets from adults diagnosed with significant KS ($Cobb\ angle = 75°$), and their corresponding biometric and spirometric values are given in Table I. Their selection to the study was done based on the medical history and the recommendation from the clinical supervisor. The measurements were effected during 2008–2009.

2) Measurements in Children: The measurements on the 33 **healthy children** were performed at the St. Vincentius Basis School in Zwijnaarde, Belgium, during 2009; the biometric details are given in Table II. The children had no history of pulmonary disease and were selected using a specific questionnaire provided by the clinical supervisor of the study. The questionnaire verified the absence of dyspnoea, chronic cough, wheeze in the chest, etc. The measurements performed on healthy children have been used to derive the respiratory impedance, and its values were compared against predicted values [13], based on their height. All measured data included in the study were validated within the 95% confidence interval values.

Asthma denotes a pulmonary disease in which there is an obstruction to the flow of air out of the lungs, but the obstruction is usually reversible, and between attacks of asthma, the flow of air through the airways is usually good [8]. Asthma is caused by chronic (ongoing, long term) inflammation of the airways, making them highly sensitive to various triggers. Asthma can be controlled using specific medication (inhaled steroids). The data for this study were recorded at the University Hospital Antwerp, during 2008–2009, from 44 asthmatic children whose corresponding biometric and spirometric values are given in Table II. Their selection for the study was based on their medical history and recommendation from the clinical supervisor. The data presented in this study have been analyzed in terms of respiratory impedance in [24].

CF is one of the most common severe (genetic) diseases, characterized by the production of abnormal secretions, leading to mucous buildup and persistent inflammation in a variety of organs [7], [14]. Inflammation and infection also cause injury and structural changes to the lungs, originating a variety of symptoms and, eventually, respiratory failure. The data used in this study were recorded at the University Hospital Antwerp during 2008–2009 from 38 data sets from children diagnosed with CF whose biometric and spirometric values are given in Table II. Their selection for the study was based on their medical history and recommendation from the clinical supervisor.

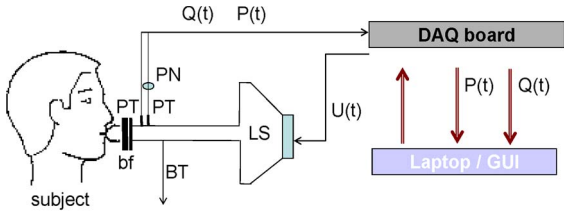

(a)

(b)

Fig. 1. (a) Schematic overview and (b) photograph of the device with a patient performing the FOT lung function test. Legend: LS—loudspeaker; BT—bias tube; PN—pneumotachograph; PT—pressure transducer; bf—biological filter with mouthpiece; Q—flow; P—pressure; $U(t)$—driving signal (test input).

B. Lung Function Testing: The FOT

The respiratory impedance was measured using the FOT standard setup, commercially available, assessing respiratory mechanics from 4 to 48 Hz in steps of 2 Hz. The subject is connected to the typical setup from Fig. 1 via a mouthpiece, suitably designed to avoid flow leakage at the mouth and dental resistance artifact. The oscillation pressure in most recent FOT devices is generated by a loudspeaker (LS) connected to a chamber, namely, the SPH-165KEP MONACOR, with a range from 3 to 1000 Hz. The LS is driven by a power amplifier fed with the oscillating signal generated by a computer, namely, a Hewlett Packard Pavilion dv1000 with a Pentium M processor, 1.5 GHz, 512 MB, with 266-MHz SDRAM. The movement of the LS cone generates a pressure oscillation inside the chamber, which is applied to the patient's respiratory system by means of a flexible respiratory tube of 1-m length and 2-cm diameter, connecting the LS chamber and the bacterial filter (bf). A side opening [bias tube (BT)] of the main tubing allows the patient to decrease the total dead space rebreathing (i.e., 40 mL). This bias tube exhibits high impedance at the excitation frequencies to avoid the loss of power from the LS pressure chamber [5]. During the measurements, the patient wears a nose clip and keeps the cheeks firmly supported to reduce the artifact of upper airway shunt.

Pressure and flow are measured at the mouthpiece, respectively, by means of the following: 1) a pressure transducer (PT) and 2) a pneumotachograph (PN) plus a differential PT. The high-precision PTs are BSDX0050D4D, with a bipolar pressure range from 0 to 1 kPa, accuracy of 0.004 kPa, and a common-mode rejection ratio of 80 dB over the frequency range of

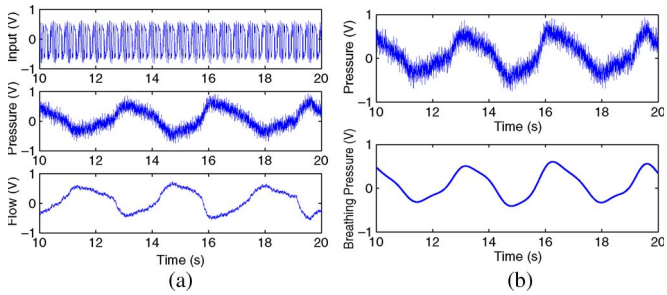

Fig. 2. (a) Typical measured signals from one subject: Oscillatory driving pressure, transrespiratory pressure, and airflow. The breathing of the patient (low frequency) can be observed superimposed on the multisine signals. (b) Typical recorded airway pressure signal from the patient and filtered breathing signal.

interest. The working range is a peak-to-peak size between 0.1 and 0.3 kPa, in order to ensure optimality and patient comfort and for the size to stay within a narrow range in order to assume linearity [33]. The flow is measured using a Hans Rudolph PN, covering a range of 0–400 L/min (6.6 L/s), 4830B series, with a dead space volume between 0 and 6.66 mL.

Averaged measurements from 3–5 technically acceptable tests were taken into consideration for further signal processing (i.e., coherence function above 0.8). The signals were acquired using a PCMCIA DAQ card 4026E series, 12 b, from National Instruments, sampled every 1 ms for periods of 15–40 s (depending on the patient's breathing limitations). Notice that the sampling time (i.e., 1 ms) is much above the highest frequency in the excitation signal (i.e., 48 Hz), providing a good measurement accuracy. Typical time records are shown in Fig. 2(a). All patients were tested in the sitting position, with cheeks firmly supported and elbows resting on the table. This lung function test has been employed in several of our earlier studies [20]–[22], [24], [25].

The output of the system is the airway pressure and flow, where both the low-frequency component (i.e., breathing) and the excitation signal (i.e., multisine) are superimposed. Since the breathing frequency is one decade below the first excited harmonic, a low-pass filter can be applied, and the breathing signal in terms of pressure and flow can be extracted. An illustrative example is shown in Fig. 2(b) in terms of breathing pressure. For the purpose of this investigation, we applied a Butterworth filter of order four and cutoff frequency at 1 Hz. For the further use of the breathing signal by means of its pressure or flow (or volume) component, an average of the full measured breathing cycles has been used. A minimum of three breathing cycles has been ensured (visually) during the measurement time, in order to have reliable information (i.e., to avoid high fluctuations from breath-to-breath variability).

C. PV Curve

In clinical terms, the air-pressure and air-volume variations in one breathing cycle plotted against each other form a closed loop known as the PV loop [32]. The area inside this loop and the slope of the axis of the minimal-to-maximal points in the PV loop are used to evaluate the respiratory mechanics of the patient. The interpretation of the PV loop is then made with respect to inspiratory and expiratory parameters, such as airflow resistance and work of breathing.

The PV loops are defined by

$$Area = \int_0^T V(t)dP(t) = \int_0^T P(t)\,dV(t) \tag{1}$$

with $P(t)$ as the pressure and $V(t)$ as the volume at time instants t. The airflow is related to the air volume by $Q(t) = dV(t)/dt$, and using this in (1), we obtain that the area is the integral of the power

$$Area = \int_0^T P(t)Q(t)\,dt \tag{2}$$

which is, by definition, the work (energy) of breathing to perform the cycle over the period T. With disease, the work of breathing is increased, and the ratio between peak pressure and peak volume is altered. However, for the purpose of this study, the area within the PV loop is of interest to us within a geometrical context. The volume has been obtained by integrating the measured airflow signal.

D. PPP Plot

Usually, it is not possible to sense all the states in a system during the experimental study of its dynamics. The classical phase-plane analysis provides information upon the dynamics of a system by means of one measured output and its derivative. However, other signals may be used to plot the phase dynamics, and these planes are then called *PPPs*. The PPP reconstruction mitigates some lack of information about the system [1], [12], [26]. The goal of the pseudophase space reconstruction is to view the signal in a higher dimensional space taking a sample measurement of its history. In order to achieve the phase space, the proper time lag T_d for the delay measurements and the adequate dimension $d \in N$ (N natural numbers) of the space must be determined. In the pseudophase space, the measured signal $s(t)$ forms the pseudovector $y(t)$ according to

$$y(t) = [s(t), s(t+T_d), \ldots, s\,(t+(d-1)T_d)]\,. \tag{3}$$

The vector $y(t)$ can be plotted in a d-dimensional space forming a curve in the pseudophase space. There is a one-to-one relationship between the data in the pseudophase space and the associated data in the true state space. If $d = 2$, we have a 2-D time-delay space (i.e., the PPP). Therefore, using the shifted signal instead of its derivative will not affect substantially the result, since the signal $\{s(t), s(t+T_d)\}$ is related by a time shift with the model $\{s(t), \dot{s}(t)\}$. More precisely, the signal $\dot{s}(t)$ is calculated using the sampling period of the measurements, whereas $s(t+T_d)$ requires a time-delay value. In resume, the PPP preserves the properties of the state space representation and characterizes the system dynamics.

Among other methods to extract PPP [30], the method of time delays is the most common method. Several techniques have been proposed to choose an appropriate time delay [1],

[26]. Usually, the average mutual information ($I_{\rm av}$) is referred as the preferred alternative to select the proper time delay T_d [12]. For the application presented in this study, we found that $I_{\rm av}$ presents a certain degree of noise and oscillations. Consequently, in order to use $I_{\rm av}$ in our study, an algorithm must be applied for smoothing the function values. Nevertheless, practice reveals that, in some cases, it is difficult to find the first minimum of $I_{\rm av}$ due to noise. Hence, a simpler low-complexity alternative solution is proposed to select the best delay T_d based on the autocorrelation of the breathing signal [12].

A better value for T_d is the value that corresponds to the first local minimum of the mutual information. On the other hand, the mutual information is a measure of how much information can be predicted about one time series point giving full information about the other. The values of T_d at which the mutual information has a local minimum are equivalent to the values of T_d at which the logarithm of the correlation sum has a local minimum. Optimal time-delay values based on the linear Pearson correlation function is a straightforward and low computational method adopted in our experiments.

Since the value of the correlation is between -1 and 1, in order to have only positive values, we take its squared value.

From the correlation function, the first local minimum is detected and denoted as the delay value T_d. Consequently, the PPP 2-D plot results from plotting the breathing pressure signal $P(t)$ on the x-axis (in volts) and the shifted breathing pressure signal $P(t+T_d)$ on the y-axis (in volts).

E. Physical Interpretation of the PV and PPP Loops

The area inside the PV loop and the slope of the axis of the minimal-to-maximal points in the PV-loop are used to evaluate the respiratory mechanics of the patient. The interpretation of the PV loop is then made with respect to inspiratory and expiratory parameters, such as airflow resistance and work of breathing.

In the phase-plane representation, we have that

$$Area = \int_0^T P(t)\cdot P(t+\tau)\,dt \tag{4}$$

with $P(t)$ as the breathing pressure signal and τ as the time delay estimated for each patient. One may notice that (4) is nothing else but the definition of the correlation function of two signals in time [27]. Since pressure and volume are related, the position of the air in the lungs is determined by each of these signals. Assuming that the pressure is a measure of the position of the air in the lungs, its delayed component is also related to the position. In this framework, we conclude that the PPP plot provides information on the position of air in the lungs between two time instants.

F. Fractal Dimension and Power-Law Model

The fractal dimension F_d is a quantity that gives an indication of how completely a spatial representation appears to fill the space. There are many specific methods to compute the fractal dimension. The most popular and simple methods are the Hausdorff dimension and the box-counting dimension [3]. The box-counting method is an iterative method. For each box size value ϵ follows a corresponding number of boxes $N(\epsilon)$ which will be needed in order to cover the area of the PPP loop. At the next iteration, another (bigger) size of the box is assumed and again used to cover the area in the PPP loop. The sequence of box sizes and their corresponding total number used cover the area of the PPP loop and will deliver a straight line on a log–log graph

$$F_d = \frac{\ln\left[N(\epsilon)\right] - \ln(C)}{\ln(1/\epsilon)} \tag{5}$$

where C is a constant related to the total area and $N(\epsilon)$ represents the minimal number of covering cells (e.g., boxes) of size ϵ required to cover the PPP graph. The slope of the straight line in the log–log plane provides the estimate of the fractal dimension F_d

$$N(\epsilon) = C(1/\epsilon)^{F_d}. \tag{6}$$

Since we have a straight line in the log–log plot, from theoretical principles of fractional calculus, it follows that a power-law model can be fitted to each group of patients [36], allowing deriving a model for each pathology

$$C = A\cdot F_d^B \tag{7}$$

with A and B as identified constants.

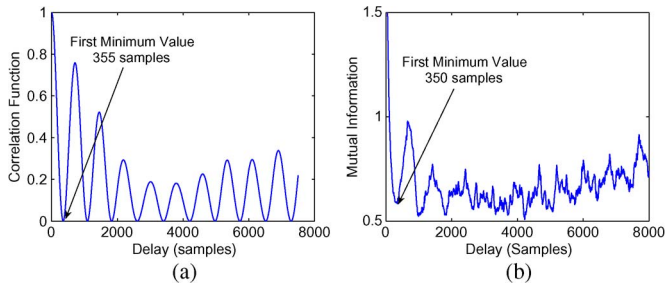

Fig. 3. Illustrative example for a healthy adult. (a) Correlation function (time delay: 355 samples). (b) Mutual information (time delay: 350 samples).

III. Results

A. PV and PPP Loops

For each measured set of signals, we have extracted the breathing signal from the pressure and flow signals by means of filtering. The volume was obtained by integrating the flow, and the PV loops were plotted for the entire signal length.

From the breathing signal extracted from the pressure signal, the time-delay value T_d was determined via the Pearson correlation function. For the sake of completeness, the mutual information has also been calculated to check that similar time-delay values are obtained as with the correlation function (e.g., 355 and 350 samples, respectively). An illustrative example for a healthy patient is shown in Fig. 3. Next, based on the extracted time-delay value, the PPP plot can be obtained. The corresponding values for the time delay are given in Table III.

TABLE III
TIME DELAY IN SAMPLES; VALUES ARE GIVEN AS MEAN ± STANDARD DEVIATION; VALUES IN BRACKETS INDICATE THE CORRESPONDING 95% CONFIDENCE INTERVALS

	mean ± std	Confidence Intervals
Healthy Adults	545 ± 185	(487,603)
COPD	798 ± 208	(733,863)
Kyphoscoliosis	352 ± 50	(330,373)
Healthy Children	373 ± 96	(339,407)
Asthma	336 ± 93	(308,365)
Cystic Fibrosis	377 ± 96	(345,408)

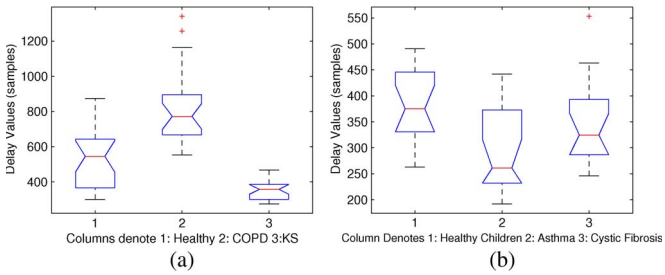

Fig. 4. ANOVA test for the calculated delay values. (a) Adult groups ($p \ll 0.001$). (b) Children groups ($p < 0.0155$).

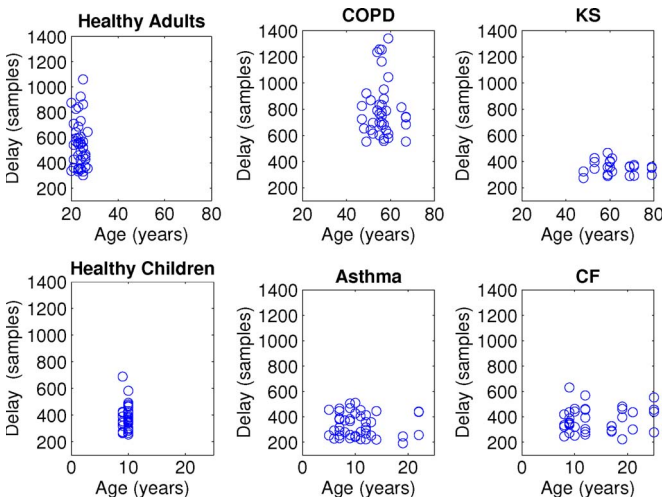

Fig. 5. Dependence of delay values with age in each group.

Fig. 4 shows the evaluation of the obtained values for the time delay by means of analysis-of-variance (ANOVA) tests (p was considered statistically significant for values lower than 0.05). Statistically significant variations have been observed between the adult groups ($p \ll 0.001$) and the children groups ($p < 0.0155$). These delay values were also verified against the biometric values of each group in order to determine if any correlation was present. The corresponding trends are shown in Fig. 5 for age. Similar results were obtained for height and weight, respectively. The dependence of the delay values with the biometric values has not been observed consistently in all the evaluated groups.

B. Fractal Dimension and Identification of Power-Law Trends

On each PV loop and PPP plot from each patient, the box-counting method was applied to obtain the fractal dimension F_d and the constant C for each patient. The models are identified

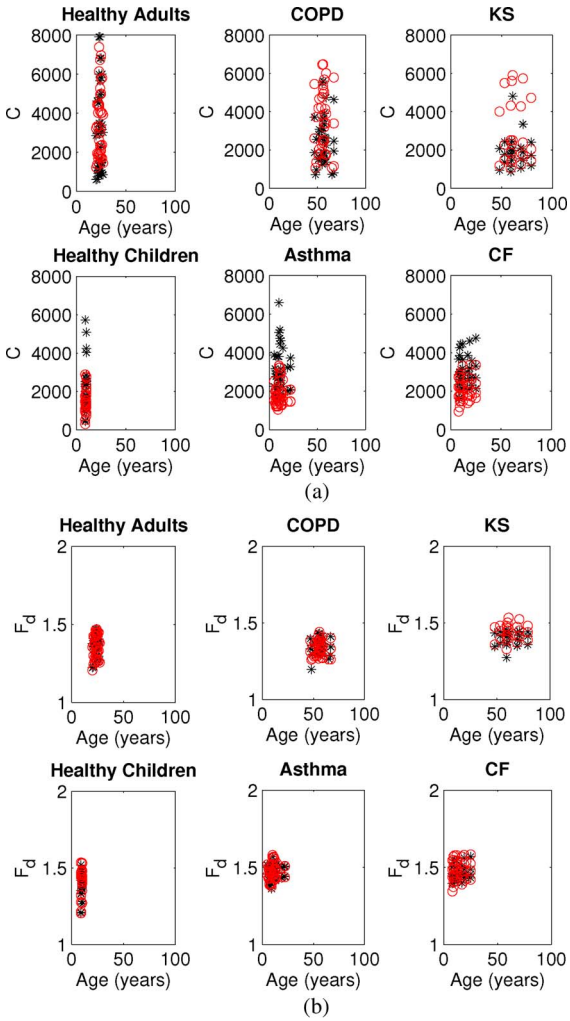

Fig. 6. Dependence with age for (a) the constant C and (b) the fractal dimension F_d. Blue stars denote the data extracted from PPP plots, while the red circles denote the data extracted from the PV plots.

for each set of measurements using the least squares algorithm [27]. Consequently, the box-counting values $N(\epsilon)$ and the box-size $1/\epsilon$ values are obtained for each patient, in each data set. The resulting data have been analyzed against biometric values in order to verify dependence, and an illustrative example is shown in Fig. 6, for the age dependence. We found no consistent dependence with age, height, and weight, respectively.

Next, the trends of the fractal dimension calculated for each group are shown in Fig. 7 by means of PV loops and in Fig. 8 by means of PPP loops, respectively. Finally, the loci of the identified power-law-model parameters from relation (7) are shown in Fig. 9, and the values are listed in Table IV.

IV. DISCUSSION

A. Relation to Dynamical Changes

In its most simple representation, the respiratory system can be represented as a series connection of a resistance R_e and a compliance C_e. It assumes that the patient's respiratory muscles are inactive and the external equipment is driving the flow into the lungs [6]. The driving pressure $P(t)$ generates flow

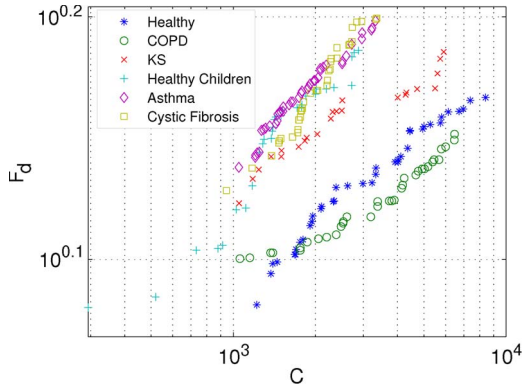

Fig. 7. Information extracted for each patient in terms of C and F_d from the PV plots.

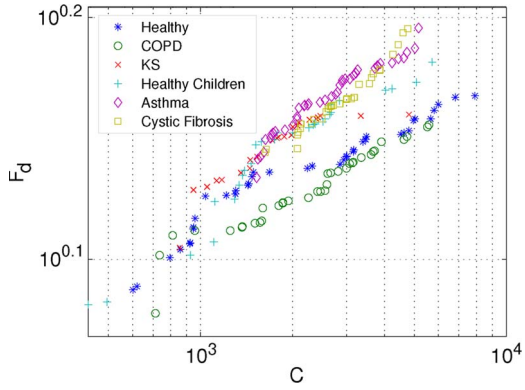

Fig. 8. Information extracted for each patient in terms of C and F_d from the PPP plots.

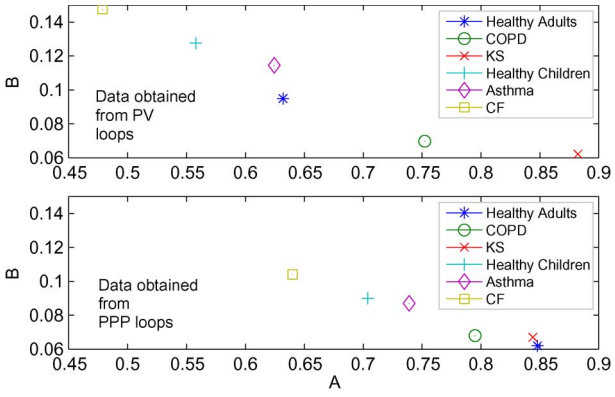

Fig. 9. Plot of the identified A and B values from model (7) for each set of data.

$Q(t)$ across the resistance, and the volume $V(t)$ changes in the compliance. If $P_r(t)$ and $P_e(t)$ are the resistive and elastic pressure drops, respectively, we have that

$$R_r = \frac{P_r(t)}{Q(t)} \quad C_r = \frac{V(t)}{P_e(t)} \quad P(t) = P_e(t) + P_r(t). \tag{8}$$

It results that

$$P(t) = R_r \cdot Q(t) + \frac{V(t)}{C_r}. \tag{9}$$

This represents the first-order equation in the motion equation for a single compartment model of the respiratory system: a single balloon with compliance C_r on a pipeline with a resistance R_r. This system can be studied using the exponential decay of volume $V(t)$ as resulting from a step input V_0: $V(t) = V_0 e^{-t/\tau}$, where t is time and τ is the time constant which characterizes the system, denoted by the product of $R_r C_r$ [19], [22], [33].

TABLE IV
FITTED POWER-LAW MODELS (7) FOR EACH GROUP OF DATA. COPD: CHRONIC OBSTRUCTIVE PULMONARY DISEASE. KS: KYPHOSCOLIOSIS. CF: CYSTIC FIBROSIS

DATA source	A PV/PPP	B PV/PPP
Healthy Adults	0.632 / 0.848	0.094 / 0.062
COPD	0.752 / 0.795	0.069 / 0.068
KS	0.882 / 0.844	0.062 / 0.067
Healthy Children	0.557 / 0.704	0.127 / 0.090
Asthma	0.624 / 0.739	0.114 / 0.087
CF	0.478 / 0.640	0.147 / 0.104

In the representation of the PPP plots, we have the breathing signal expressed as pressure and its time-delayed derivative. From (9), it can be observed that there exists a relation between pressure and flow $(Q(t) = dV/dt)$. In clinical terms, the PV loop during one breathing period is able to tell the clinician something about the dynamic compliance of the respiratory system and its work. The area enclosed by the PV loop is called the physiologic work of breathing, denoting the resistive work performed by the patient to overcome the resistance present in the airways. The mathematical description has been given in Section II-E.

During cycling loading, the stress that develops in the viscoelastic body (respiratory tissue) displays the following:

1) a component in phase with strain, which is the elastic stress contributing to the storage modulus E_S (elastance);
2) a component out of phase with strain, corresponding to the viscous dissipation and contributing to the loss modulus E_D (damping).

In [10] and [23], it was shown that the respiratory system can be indeed modeled as a combination of series RC elements in a cascade arrangement of consecutive airways, by using their mechanical analog representation, springs K_{rs}, and dashpots B_{rs}. In this mechanical model, it follows that the PV relationship equivalent to the stress–strain relationship is given by

$$P(t) = \frac{K_{rs}\ell_{rs}}{A_{rs}} V(t) + \frac{B_{rs}\ell_{rs}}{A_{rs}} \frac{dV(t)}{dt} \tag{10}$$

with P as the air pressure, V as the air volume, ℓ_{rs} and A_{rs} as the changes in length and area of airways during the breathing cycle, and K_{rs} and B_{rs} as the constants of the spring and dashpot, respectively [10]. This relation suggests that the PPP loop is a measure of the mechanical properties in the lung parenchyma and airways during breathing. The respiratory mechanical properties have been shown to be related to the structure of the lungs, which, consequently, is altered by pathology [19], [23].

Normal quiet breathing (such as during the FOT lung function test) is accomplished by contraction of the diaphragm, the parasternal muscles, and the scaleni. During inspiration, the diaphragm pulls the lower surfaces of the lung downward.

Expiration results from simple relaxation of these muscles. Changes in the elastic recoil of the lungs (more, or less, stiffness) will affect their normal function, in particular, total lung volume and PV relationships.

B. Relation to Structural Changes

It has been recognized that the structure of the respiratory tree is strongly related to that of fractal structures [41]. Moreover, it has been shown that the particular dichotomous structure is a necessity for optimality with respect to total volume and resistance [16], [41]. The morphology of the human tree provides maximal efficiency in assuring air distribution with minimal viscous dissipation. The geometrical and morphological structure of the healthy lung has been shown to lead to lumped models of fractional order derivatives and integrals [19], [22], which are, by definition, models for systems with long-memory properties (e.g., the respiratory system).

In [28], it has been shown that the structure and its bifurcating geometry play an important role in ventilation. Assuming a ratio h between diameter and length between two consecutive airway generations—the homothety factor—the authors have shown that the volume and pressure drop can be written as

$$V_N = V_0 \left[1 + \sum_{i=1}^{N} (2h^3)^i\right] \tag{11}$$

$$\Delta P_N = R_0 \bar{Q} \left[1 + \sum_{i=1}^{N} \frac{1}{(2h^3)^i}\right] \tag{12}$$

respectively, with $\bar{Q}$ as the global airflow, R_0 and V_0 as some initial values for resistance and volume, respectively, i as the airway generation number, and N as the total number of airway generations in the respiratory tree. The validity of these relations has been shown to be true for the lower part of the bronchial tree (i.e., generations 6–16). Since the same factor $(2h^3)^i$ appears in both equations, there is an interplay between pressure and volume values. The fractal dimension in terms of lung structure is given by

$$FD_s = \frac{\log 2}{\log(1/h)}. \tag{13}$$

For a realistic respiratory tree, the assumption of a fractal structure does not hold. Nevertheless, it has been shown that, although the structure is random, with different reduction ratios in a dichotomous bifurcation, the total resistance is given by

$$R_N = R_0 \left[1 + \sum_{i=1}^{N} \left(\frac{1}{h_1^3 + h_2^3}\right)^i\right] \tag{14}$$

with h_1 and h_2 as the homothety factors for the left and right branches, respectively. The critical value for the lungs is given by $h = 0.85$, corresponding to a low resistance and volume higher than necessary [41]. This value is higher than the value $h = 0.79$ for the symmetric model [28]. The relation (14) gives the homothety factor of $h = 0.76$, which is close to that given by the symmetrical structure model. Hence, it follows that the resistance depends on the structure and *not on the degree of symmetry*. Since the value of $0.85 > 0.79$, it follows that the design of the lungs is made with a safety margin for breathing in conditions of bronchial constriction [28].

The structural changes in the respiratory tree will change the value of the homothety factor h, and one can analyze the dynamics of the respiratory tree in terms of pressure and volume variations. If the homothety factor decreases from "optimal," then an increase in the pressure drop will occur (higher effort to breath). If the homothety factor increases from "optimal," the resistance is small, i.e., the volume will increase for lower pressure drop values.

In asthma, the inner diameters of the bronchioli, and not their length, are reduced. In this case, the airway ducts are no longer homothetic, and the diameter and length of the sequential bronchioles are altered. This implies that the pressure drop is given by

$$\Delta P_N = R_0 \bar{Q} \left[1 + \sum_{i=1}^{N} \frac{1}{2^i} \frac{h_1}{(h_d^4)^i}\right] \tag{15}$$

with h_1 as the length reduction ratio and h_d as the diameter reduction ratio. The nonlinear effect of the constriction is more pronounced, since a small reduction in h_d will have a manifold effect in the total tree resistance.

The fractal dimension extracted from the PV and PPP loops is indirectly related to the structure of the respiratory tree, since it quantifies the work of breathing, a measure of the combined effect of pressure and volume. This implies that, indirectly, the proposed methods in this paper offer a measure of the degree of homothety in the lungs. In other words, we indirectly evaluate the degree of optimality in the respiratory process.

From Table IV, we observe that the values identified from mapping the information obtained in the PV loops provide more consistent results than those given by the PPP plots. Indeed, from Fig. 9, one can observe that the identified values for (7) are more dispersed in the context of PV loop, allowing a clearer separation between the groups. The data for the adults and the children do not overlap; thus, the validity of the results is supported. In terms of the A parameter, its value for the adult group seems to be correlated directly with the airway resistance. Its values are increasing with COPD and KS, which corresponds to the clinical pathology. For the children group, its values are close to each other for healthy and asthma. We suspect that the reason might be the medication taken by the asthmatic patients, which had mostly normal-to-the-exam spirometric values (i.e., controlled asthma). The values for the children with pulmonary CF were lower than those in healthy, indicating a lower resistance, either by means of lower pressure drop or by means of higher volume. In terms of the B parameter, its value seems to be correlated inversely with the resistance or directly with the volume. The values in COPD and KS were lower, indicating lower volumes, which corresponds to the clinical pathology. In children, the values of healthy and asthma were again close to each other, while in CF patients, the values were higher (i.e., higher values). We conclude that the values for the CF group might be subject to the weight and height biometric parameters.

C. Limitations

One of the limitations of the study is that the groups of subjects and patients were not equally balanced in terms of male/female distribution; hence, dependence with gender was not determined. Similarly, dependence may exist for the adult groups in terms of age. The healthy adult group had an averaged age value significantly lower than those diagnosed with COPD and KS. The dependence with height and weight was not consistently observed in all groups; hence, we could not conclude whether these biometric parameters will influence our results. However, even if this is the case, the seminal ideas presented in this work still hold, in the sense that there exists a link between changes in the structure and dynamic patterns in the breathing.

We have also concluded that the PV loop provides better results than PPP loop in terms of separation of the groups. However, the PV loop requires the recording of two signals: pressure and flow or, similarly, pressure and volume. In the context of FOT, there is a twenty-five-fold difference in the cost of pressure sensors and flow sensors. Therefore, measuring only one signal may be an interesting approach to support the use of PPP plots instead of PV plots. The advantage would be that, if the pressure is available (i.e., the cheapest measurement), then the delayed derivative of pressure can be used to plot the PPP.

From a clinical standpoint, we have shown that one of the proposed parameters (i.e., A) is related to the resistive components of the breathing dynamics as extracted from the PPP loops. However, we do not yet have a parameter which characterizes the elastic components. Also, there is no information as to how the inhomogeneities in the lung affect the results of the PPP loops. We conclude that, in order to provide a concise interpretation and mapping of the short-term breathing dynamics by means of PPP plots, a bigger database of patient data must be analyzed.

V. Conclusion

In this paper, the analysis of tidal breathing patterns measured during noninvasive forced oscillation lung function tests has been applied to adult and children groups. The adult groups were healthy, with prediagnosed COPD, and with prediagnosed KS, respectively. The three children groups were healthy, with prediagnosed asthma, and with prediagnosed CF, respectively. The fractal dimension has been evaluated from the area determined by the PV curves and the PPP loop by means of the box-counting method. The results indicate the existence of a relation between the area of the loops, power-law patterns, and alterations in the respiratory structure with disease. We obtained statistically significant variations between the data sets corresponding to the six groups of patients, showing that classification between the groups can be obtained by means of the proposed method. Our findings support the idea that the respiratory system changes with disease in terms of airway geometry and tissue parameters, leading, in turn, to variations in the fractal dimension of the airway structure and of the dynamic pattern of breathing.

Acknowledgment

The authors would like to thank the technical assistance provided at the University of Pharmacology and Medicine–"Leon Daniello" Hospital, Cluj-Napoca, Romania, to measure COPD-diagnosed patients; University Hospital Ghent, Belgium, to measure KS-diagnosed patients; and University Hospital Antwerp, Belgium, to measure asthma and CF-diagnosed children. The authors would also like to thank the anonymous reviewers, whose comments helped substantially to improve the technical quality of this paper. Author C. M. Ionescu would like to thank the volunteers from Ghent University, Ghent, Belgium, and from the primary school in Zwijnaarde who performed the lung function testing in our laboratory.

References

[1] H. D. I. Abarbanel, R. Brown, J. Sidorowich, and L. Tsimring, "The analysis of observed chaotic data in physical systems," *Rev. Modern Phys.*, vol. 65, no. 4, pp. 1331–1392, Oct.–Dec. 1993.

[2] P. J. Barnes, "Chronic obstructive pulmonary disease," *NEJM Med. Progr.*, vol. 343, no. 2, pp. 269–280, 2000.

[3] G. L. Baker and J. B. Gollub, *Chaotic Dynamics: An Introduction*, 2nd. Cambridge, U.K.: Cambridge Univ. Press, 1996.

[4] J. Bates, "A recruitment model of quasi-linear power-law stress adaptation in lung tissue," *Ann. Biomed. Eng.*, vol. 35, no. 7, pp. 1165–1174, Jul. 2007.

[5] M. Birch, D. MacLeod, and M. Levine, "An analogue instrument for the measurement of respiratory impedance using the forced oscillation technique," *Phys. Meas.*, vol. 22, no. 2, pp. 323–339, May 2001.

[6] J. Blom, *Monitoring of Respiration and Circulation*. Boca Raton, FL: CRC Press, 2004.

[7] S. Brennan, G. Hall, F. Horak, A. Moeller, P. Pitrez, A. Franzamann, S. Turner, N. de Clerck, P. Franklin, K. Winfield, E. Balding, S. Stick, and P. Sly, "Correlation of forced oscillation technique in preschool children with cystic fibrosis with pulmonary inflammation," *Thorax*, vol. 60, no. 2, pp. 159–163, Feb. 2005.

[8] W. Busse and R. Lemanske, "Asthma," *New Engl. J. Med.*, vol. 344, no. 5, pp. 350–362, Feb. 2001.

[9] W. H. Deng, C. P. Li, and J. Lü, "Stability analysis of linear fractional differential system with multiple time-delays," *Nonlinear Dyn.*, vol. 48, no. 4, pp. 409–416, Jun. 2007.

[10] N. De Geeter, C. Ionescu, and R. De Keyser, "A mechanical model of soft biological tissue—An application to lung parenchyma," in *Proc. 31st Annu. Int Conf. IEEE Eng. Med. Biol. Soc.*, Minneapolis, MN, ISBN 978-1-4244-3296-7, Sep. 2–6, 2009, pp. 2863–2866.

[11] R. D. Driver, "Ordinary and delay differential equations," in *Applied Mathematical Sciences*. New York: Springer-Verlag, ISBN 0-387-90231-7, 1977.

[12] F. Duarte, J. A. Tenreiro Machado, and G. Duarte, "Dynamics of the Dow Jones and the NASDAQ stock indexes," *Nonlinear Dyn.*, vol. 61, no. 4, pp. 691–705, Sep. 2010, DOI: 10.1007/s11071-010-9680-z.

[13] E. Duiverman, J. Clement, K. Van de Woestijne, H. Neijens, A. van den Bergh, and K. Kerrebijn, "Forced oscillation technique: Reference values for resistance and reactance over a frequency spectrum of 2–26 Hz in healthy children aged 2.3–12.5 years," *Clin. Respiratory Physiol.*, vol. 21, no. 2, pp. 171–178, Mar. 1985.

[14] A. Elizur, C. Cannon, and T. Ferkol, "Airway inflammation in cystic fibrosis," *Chest*, vol. 133, no. 2, pp. 489–495, Feb. 2008.

[15] B. Faybishenko, "Nonlinear dynamics in flow through unsaturated fractured porous media: Status and perspectives," *Rev. Geophys.*, vol. 42, p. RG2003, Jun. 2004, DOI: 10.1029/2003RG000125.

[16] C. Hou, S. Gheorgiu, M. O. Coppens, V. Huxley, and P. Pfeifer, "Gas diffusion through the fractal landscape of the lung: How deep does oxygen enter the alveolar system?" in *Fractals in Biology and Medicine*, G. Losa, D. Merlini, T. Nonnenmacher, and E. R. Weibel, Eds. Berlin, Germany: Birkhaüser, 2005, pp. 17–30.

[17] R. L. Hughson, Y. Yamamoto, and J. O. Fortrat, "Is the pattern of breathing at rest chaotic? A test of the Lyapunov exponent," *Adv. Exp. Med. Biol.*, vol. 393, pp. 15–19, 1995.

[18] R. L. Hughson, Y. Yamamoto, J. O. Fortrat, R. Leask, and M. S. Fofana, "Possible fractal and/or chaotic breathing patterns in resting humans,"

in *Bioengineering Approaches to Pulmonary Physiology and Medicine*, M. C. K. Khoo, Ed. New York: Plenum, 1996, pp. 187–196.
[19] C. Ionescu, P. Segers, and R. De Keyser, "Mechanical properties of the respiratory system derived from morphologic insight," *IEEE Trans. Biomed. Eng.*, vol. 56, no. 4, pp. 949–959, Apr. 2009.
[20] C. Ionescu, R. De Keyser, K. Desager, and E. Derom, "Fractional-order models for characterizing the impedance of the respiratory system," in *Advances in Biomedical Engineering*, vol. 9, G. Naik, Ed. Rijeka, Croatia: In-Tech Publishing House, 2009, pp. 377–396, ISBN 978-953-307-004-9. [Online]. Available: www.intechweb.org/books.php
[21] C. Ionescu, E. Derom, and R. De Keyser, "Assessment of respiratory mechanical properties with constant-phase models in healthy and COPD lungs," *Comput. Methods Programs Biomed.*, vol. 97, no. 1, pp. 78–85, Jan. 2010.
[22] C. Ionescu, I. Muntean, J. T. Machado, R. De Keyser, and M. Abrudean, "A theoretical study on modeling the respiratory tract with ladder networks by means of intrinsic fractal geometry," *IEEE Trans. Biomed. Eng.*, vol. 57, no. 2, pp. 246–253, Feb. 2010.
[23] C. Ionescu, W. Kosinsky, and R. De Keyser, "Viscoelasticity and fractal structure in a model of human lungs," *Arch. Mech.*, vol. 62, no. 1, pp. 21–48, 2010.
[24] C. Ionescu, K. Desager, and R. De Keyser, "Fractional order model parameters for the respiratory input impedance in healthy and in asthmatic children," *Comput. Methods Programs Biomed.*, vol. 101, no. 3, pp. 315–323, Mar. 2011, DOI: 10.1016/j.cmpb.2010.11.010.
[25] C. Ionescu, J. Tenreiro-Machado, and R. De Keyser, "Is multidimensional scaling suitable for mapping the input respiratory impedance in subjects and patients?" *Comput. Methods Programs Biomed.*, vol. 104, no. 3, pp. e189–e200, Dec. 2011.
[26] M. Lima, J. A. Tenreiro Machado, and M. Crisóstomo, "Pseudo phase plane, delay and fractional dynamics in robotic signals," *JESA, J. Eur. Syst. Autom.—Special Issue on Fractional Differentiation*, vol. 42, no. 6–8, pp. 1037–1051, 2008.
[27] L. Ljung, *System Identification: Theory for the User*. Upper Saddle River, NJ: Prentice-Hall, 1999.
[28] B. Mauroy, M. Flloche, E. R. Weibel, and B. Sapoval, "An optimal bronchial tree may be dangerous," *Nature*, vol. 427, no. 6975, pp. 633–636, Feb. 2004.
[29] F. McCool and D. Rochester, "Non-muscular diseases of the chest wall," in *Fishman's Pulmonary Disease and Disorders*, A. Fishman, Ed. New York: McGraw-Hill Med., 2008, pp. 1541–1548.
[30] F. C. Moon, *Chaotic Vibration*. New York: Wiley, 1987.
[31] A. Monje, Y. Chen, B. Vinagre, D. Xue, and V. Feliu, *Fractional Order Systems and Controls*. London, U.K.: Springer-Verlag, 2010.
[32] R. Northrop, *Non-Invasive Instrumentation and Measurement in Medical Diagnosis*. Boca Raton, FL: CRC Press, 2002.
[33] E. Oostveen, D. Macleod, H. Lorino, R. Farré, Z. Hantos, K. Desager, and F. Marchal, "The forced oscillation technique in clinical practice: Methodology, recommendations and future developments," *Eur. Respiratory J.*, vol. 22, no. 6, pp. 1026–1041, Dec. 2003.
[34] H. Pasker, M. Peeters, P. Genet, N. Nemery, and K. Van De Woestijne, "Short-term ventilatory effects in workers exposed to fumes containing zinc oxide: Comparison of forced oscillation technique with spirometry," *Eur. Respiratory J.*, vol. 10, no. 7, pp. 1523–1529, Jul. 1997.
[35] C.-K. Peng, J. Mietus, Y. Liu, C. Lee, J. Hausdorff, H. Stanley, A. Goldberger, and L. Lipsitz, "Quantifying fractal dynamics of human respiration: Age and gender effects," *Ann. Biomed. Eng.*, vol. 30, no. 5, pp. 683–692, May 2002.
[36] I. Podlubny, "Geometrical and physical interpretation of fractional integration and fractional differentiation," *J. Fract. Calculus Appl. Anal.*, vol. 5, no. 4, pp. 357–386, 2002.
[37] P. Quanjer, "Referentiewaarden," in *Longfunktie Onderzoek*, M. Demedts and M. Decramer, Eds. Leuven, Belgium: Garant, 1998, pp. 27–37.
[38] B. Suki, A. L. Barabasi, and K. Lutchen, "Lung tissue viscoelasticity: A mathematical framework and its molecular basis," *J. Appl. Physiol.*, vol. 76, no. 6, pp. 2749–2759, Jun. 1994.
[39] J. A. Tenreiro Machado, "Analysis and design of fractional-order digital control systems," *J. Syst. Anal.-Modell.-Simul.*, vol. 27, no. 2/3, pp. 107–122, 1997.
[40] J. A. Tenreiro Machado, "A probabilistic interpretation of the fractional-order differentiation," *J. Fract. Calculus Appl. Anal.*, vol. 6, no. 1, pp. 73–80, 2003.
[41] E. R. Weibel, "Mandelbrot's fractals and the geometry of life: A tribute to Benoít Mandelbrot on his 80th birthday," in *Fractals in Biology and Medicine*, G. Losa, D. Merlini, T. Nonnenmacher, and E. R. Weibel, Eds. Berlin, Germany: Birkhaüser, 2005, pp. 3–16.
[42] B. West (2010). Fractal physiology and the fractional calculus: A perspective. *Frontiers Fractal Physiol.* [Online]. *1(12)*, pp. 1–17. Available: www.frontiersin.org

Clara M. Ionescu (S'06–M'09) was born in Cimpulung, Romania, in 1979. She received the M.Sc. degree in industrial informatics and automation from "Dunarea de Jos" University, Galati, Romania, in 2003 and the Ph.D. degree from Ghent University, Ghent, Belgium, in 2009, on identification of human respiratory system by means of fractional order models.

She is currently a Postdoctoral Fellow with Ghent University, involved in several international projects, with both industrial and biomedical applications, for identification and control.

Dr. Ionescu was a recipient of the Postdoctoral Fellowship Grant from the Research Foundation Flanders (FWO). She has about 100 peer-reviewed publications in journals, conferences, and books, being actively involved in promoting the concept of fractality in biological systems and their applications to medicine.

J. A. Tenreiro Machado (M'07–SM'10) was born in 1957. He received the "Licenciatura," Ph.D., and "Habilitation" degrees in electrical and computer engineering from the University of Porto, Porto, Portugal, in 1980, 1989, and 1995, respectively.

During 1980–1998, he was a Professor with the Department of Electrical and Computer Engineering, University of Porto. Since 1998, he has been a Coordinator Professor with the Department of Electrical Engineering, Porto Superior Institute of Engineering, Polytechnic Institute of Porto. His main research interests are fractional calculus, nonlinear dynamics, modeling, control, robotics, intelligent transportation systems, and evolutionary computing.

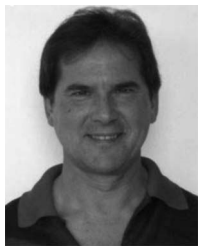

Robin De Keyser received the M.Sc. degree in electromechanical engineering and the Ph.D. degree in control engineering from Ghent University, Ghent, Belgium, in 1974 and 1980, respectively.

He is currently a Full Professor of control engineering with the Faculty of Engineering, Ghent University. He is the author/coauthor of about 300 publications in journals, books, and conference proceedings. He acted as an External Review Expert in several European Commission research programs and is one of the pioneers who produced the original concepts of predictive control during the 1980s. His teaching and research activities include model predictive control, autotuning and adaptive control, modeling and simulation, and system identification. His research is application driven, with many pilot implementations in technical and nontechnical systems, such as chemical, steel, marine, mechatronic, semiconductor, power electronics, and biomedical.